We are IntechOpen, the world's leading publisher of Open Access books Built by scientists, for scientists

4,800
Open access books available

122,000
International authors and editors

135M
Downloads

Our authors are among the

154
Countries delivered to

TOP 1%
most cited scientists

12.2%
Contributors from top 500 universities

CLARIVATE ANALYTICS BOOK CITATION INDEX INDEXED

WEB OF SCIENCE™

Selection of our books indexed in the Book Citation Index in Web of Science™ Core Collection (BKCI)

Interested in publishing with us?
Contact book.department@intechopen.com

Numbers displayed above are based on latest data collected.
For more information visit www.intechopen.com

16

Targeting EGFR and HER2 for Molecular Imaging of Cancer

Haibiao Gong, Lakshmi Sampath,
Joy L. Kovar and D. Mike Olive
LI-COR Biosciences, Lincoln, USA

1. Introduction

The epidermal growth factor (EGF) receptor (EGFR, HER1, ErbB1) and human epidermal growth factor receptor type 2 (HER2, ErbB2) belong to the ErbB family of type I tyrosine kinases (TKs). This family of receptor TKs also includes another two closely related members HER3/ErbB3 and HER4/ErbB4. The general structure of these cell surface receptor proteins contains an extracellular ligand-binding domain, a hydrophobic transmembrane domain, an intracellular tyrosine kinase domain and a non-catalytic carboxyl terminal tail (Ferguson et al., 2000; Kari et al., 2003; Mitsudomi & Yatabe, 2010; Pines et al., 2010). Various ligands for EGFR, HER3 and HER4 have been identified, with EGF the most extensively characterized for its binding and activation of EGFR. These ErbB proteins are present in the plasma membrane as monomers. Upon ligand binding, the ErbB receptors can associate with each other to form different receptor dimers, which may be homodimers (e.g., EGFR-EGFR) or heterodimers (e.g., EGFR-HER2). The dimerization results in the activation of kinase activity and downstream signaling pathways, which often leads to cell proliferation and malignant tumor growth. HER2 is an exception, with no compatible ligand identified. However, it is the preferred heterodimerization partner for all other ErbB members (Mishani & Hagooly, 2009; Niu et al., 2008; Tzahar et al., 1996; Yarden & Sliwkowski, 2001).

As EGFR and HER2 play important roles in many physiological and pathological processes, it is not surprising that deregulation of EGFR and HER2 is associated with various types of malignancies (Kari et al., 2003; Niu et al., 2008; Yarden & Sliwkowski, 2001). Both overexpression and mutation of EGFR have been identified in various types of cancers, while overexpression is a more commonly employed mechanism in the case of HER2 (Yarden & Sliwkowski, 2001). In these cancer cells, the TK activity is either elevated or constitutively activated. EGFR- and HER2-targeted anti-cancer medicines have been developed by either targeting the extracellular ligand-binding domain through antibody blocking, or by inhibiting the tyrosine kinase activity using low-molecular-weight molecules (Baselga, 2006; Pines et al., 2010; Speake et al., 2005). Cetuximab (a humanized mouse antibody) and panitumumab (a fully human antibody) have been approved for selected EGFR-targeted cancer treatment. Although these antibodies are designed to down-regulate EGFR signaling by inhibiting ligand-binding, preventing receptor dimerization and

accelerating receptor degradation, antibody-dependent cell-mediated cytotoxicity is also considered as an important mechanism for IgG1 isotype antibody cetuximab (Cai et al., 2008; Okamoto, 2010). Trastuzumab (a humanized mouse antibody) is a widely used treatment for breast cancer patients with HER2 overexpression (Niu et al., 2008). Because TKs depend on ATP to provide phosphate for the phosphorylation process, small molecules that bind to the ATP-binding pocket of the kinase domain can inhibit its enzymatic activity. These TK inhibitors (TKIs) may bind either reversibly or irreversibly. Reversible TKIs erlotinib and gefitinib are EGFR-specific, while lapatinib inhibits both EGFR and HER2 (Pines et al., 2010).

Molecular imaging agents with specific targets can provide information regarding biological processes at a cellular level before anatomical changes occur. Similar to the approaches used to develop EGFR and HER2 therapeutic agents, two strategies could be used for EGFR- and HER2-targeted tumor imaging. The first class of imaging agents targets extracellular domain of the receptor. Examples of these imaging agents include whole antibodies, antibody fragments, affibodies and nanobodies. The EGFR ligands, which bind to EGFR extracellular domain at high affinity, could also be used for this purpose. The second class of molecules includes TKIs and analogs that bind reversibly or irreversibly to the kinase domain of the receptor. Actually, some of the EGFR- and HER2-targeted therapeutic agents mentioned above have been used for tumor imaging after labeling with different functional groups, such as radionuclides for positron emission tomography (PET) and single-photon emission computed tomography (SPECT) imaging, and fluorescent dyes for optical imaging (Mishani et al., 2008; Mishani & Hagooly, 2009; Niu et al., 2008).

2. Imaging agents targeting EGFR

2.1 Anti-EGFR antibodies

PET imaging with ^{64}Cu ($t_{1/2}$ = 12.7 h)-labeled cetuximab (^{64}Cu-DOTA-cetuximab) was employed to measure the EGFR expression in seven xenograft tumor models *in vivo*. The data was compared with EGFR levels in the tumors determined by Western blot. A reasonable linear correlation (R^2 = 0.80) between the tumor uptake of ^{64}Cu-DOTA-cetuximab (measured by PET) and the EGFR protein expression level (measured by Western blot) was discovered. It was also found that ^{64}Cu-DOTA-cetuximab had increasing tumor accumulation over time in EGFR-positive tumors but relatively low uptake in EGFR-negative tumors (Cai et al., 2007). In a following study, ^{64}Cu-DOTA-cetuximab was used to monitor the early response of EGFR degradation induced by 17-allyamino-17-demethoxygeldanamycin (17-AAG) treatment (Niu et al., 2008). 17-AAG is an Hsp90 inhibitor, which induces the degradation of EGFR protein (Lang et al., 2007). In a PC-3 prostate tumor model, 17-AAG treatment induced significant reduction of ^{64}Cu-DOTA-cetuximab uptake in the tumor. The reduction of ^{64}Cu-DOTA-cetuximab uptake correlated well with the lower EGFR protein level in the treated tumor as determined by immunofluorescence staining and Western blot (Niu et al., 2008).

Cetuximab has also been labeled with fluorescent dyes for optical imaging. Cy5.5 (Ex/Em: 675/695 nm)-labeled cetuximab (cetuximab-Cy5.5) was taken up specifically by head and neck squamous cell carcinoma (HNSCC) xenografts. The fluorescence from mouse tumors treated with cetuximab-Cy5.5 was significantly higher compared to a control probe IgG1-

Cy5.5 (Rosenthal et al., 2007). To reduce the background fluorescence signal, a two-step activation strategy was designed. EGFR-overexpressing tumors (A431) were pre-targeted with biotinylated cetuximab, followed by administration of neutravidin conjugated with BODIPY-FL fluorescent dye (nAv-BDPfl). As the fluorescence of nAv-BDPfl increases dramatically (~ 10-fold) upon binding to biotin, the nAv-BDPfl signal will be specifically activated at the tumor site, where the biotinylated cetuximab was concentrated. Not surprisingly, this approach produced a higher tumor-to-background ratio (Hama et al., 2007). Another activatable probe employed the fluorescence quenching of ICG after conjugation with antibodies. The fluorescence could be restored by disrupting the molecular interaction between ICG and antibodies either *in vitro* (SDS plus 2-ME treatment) or *in vivo* (target binding and internalization). ICG-labled panitumumab (labeling ratio 1:5) exhibited a 58-fold signal increase upon SDS/2-ME treatment. EGFR-overexpressing tumors (A431 and MDA-MB-468) could be identified by this probe. Two other antibodies, trastuzumab (anti-HER2) and daclizumab (anti-CD25) were also labeled with ICG and used to image their respective targets in this study (Ogawa et al., 2009).

In an attempt to extend EGFR-targeted imaging with cetuximab to clinical scenario, cetuximab was labeled with ^{99m}Tc ($t_{1/2}$ = 6 h). The resulting imaging probe ^{99m}Tc-EC-C225 was evaluated by cell uptake assay, and in tumor-bearing mice and rats. SPECT imaging on a patient with squamous cell carcinoma visualized the tumor 2 h after ^{99m}Tc-EC-C225 administration (Schechter et al., 2003). Assessment of the radiation dosimetry of this probe indicated that it has reasonable dosimetric properties for a diagnostic nuclear medicine agent (Schechter et al., 2004).

EGFR variant III (EGFRvIII) is a common in-frame deletion mutant that lacks a large part of the extracellular portion (exons 2-7), including components of the ligand-binding domain (Ekstrand et al., 1992). EGFRvIII is constitutively activated, and associated with glioblastoma and some other tumors, such as prostate and breast cancer (Wikstrand et al., 1998). EGFRvIII could be recognized by ch806, a chimeric anti-EGFR antibody that selectively binds an EGFR epitope exposed only on mutant, overexpressed, or ligand-activated forms of the receptor (Panousis et al., 2005). ^{124}I ($t_{1/2}$ = 4.2d)-labeled ch806 (^{124}I -IMP-R4-ch806) was able to detect EGFRvIII expressing tumors (U87MG.EGFRvIII) at 24 h after probe injection, and prolonged retention was evident up to 168 h post-injection. There was a good correlation between *in vivo* tumor PET quantitation of ^{124}I -IMP-R4-ch806 and *ex vivo* measurement from dissected tissues. Remarkably, this probe was tumor-specific, and no significant binding to normal tissue was observed (Lee et al., 2010). This is in contrast to cetuximab, which accumulates in EGFR-expressing tissues such as liver (Niu et al., 2008).

2.2 EGFR-specific antibody fragments

Due to their large size (~150 kDa), the antibody-based imaging agents suffer from drawbacks such as long biodistribution time, poor penetrating capability, and slow clearance from the blood and normal tissues, which causes limited imaging contrast early post-injection, high background signal and non-uniform tumor penetration (Gong et al., 2010; Schier et al., 1996). Antibodies could be dissected into minimal monovalent binding fragments, such as Fab (~55 kDa) and scFv (~28 kDa), which retain the binding specificity (Holliger & Hudson, 2005). These antibody fragments have also been used for molecular imaging studies.

The Fab fragment of a fully human antibody that recognizes the native extracellular domain of EGFR was labeled with ^{125}I ($t_{1/2}$ =59.4 d). The binding of ^{125}I-Fab to EGFR was confirmed by immunoprecipitation (IP) and fluorescence-activated cell sorting (FACS). In an animal imaging study, ^{125}I-Fab was able to distinguish the tumors with different levels of EGFR expression (Xu et al., 2009). An EGFR-specific scFv was isolated from a phage display library, and labeled with either quantum dot (QD) for fluorescence imaging, or magnetic iron oxide (IO) for magnetic resonance imaging (MRI). The resulting EGFR-targeted nanoparticles were discovered to accumulate in pancreatic xenograft tumors by tissue section fluorescence imaging and whole animal MRI (Yang et al., 2009). To achieve site-specific labeling, an anti-EGFR scFv was fused to the SNAP-tag creating a fusion protein 425(scFv)SNAP (~48 kDa) (Kampmeier et al., 2010). SNAP-tag is a 20-kDa protein derived from the human DNA repair protein O^6-alkylguanine-DNA-alkyltransferase (hAGT), which reacts with the fluorescent dye conjugated benzylguanine (BG) substrate, leading to covalent labeling of the fluorescent dye on the fusion protein (Keppler et al., 2004). The fusion protein 425(scFv)SNAP labeled with the near-infrared (NIR) substrate BG-747 accumulated rapidly and specifically at the tumor site. Due to the efficient clearance, the tumor to background ratio (TBR) of this probe was significantly higher compared to the full-length antibody cetuximab (Kampmeier et al., 2010).

Camelids contain a unique type of antibodies lacking the light chain (Hamers-Casterman et al., 1993). The single variable domain of heavy chain (VHH) has been isolated, and termed nanobody (~15 kDa). Several EGFR-specific nanobodies were labeled with ^{99m}Tc for SPECT imaging. These ^{99m}Tc-lableded nanobody molecules showed high specificity towards EGFR-overexpressing A431 tumors. The clearance from the blood was fast. The probe accumulation in the kidney was much higher than that in the liver, indicating a kidney clearance route (Gainkam et al., 2008; Huang et al., 2008). We labeled an EGFR-specific nanobody molecule (a kind gift from Dr. Paul van Bergen en Henegouwen at Utrecht University) with a NIR fluorescent dye IRDye® 800CW (Ex/Em: 774/789 nm) and used it for *in vivo* optical imaging. A431 xenograft tumors could be clearly identified at 1d post-injection with different dosages (0.4, 0.8 and 1.6 nmol per mouse) (Fig. 1). Consistent with SPECT results, the kidney accumulation of this fluorescent probe was high (Gong *et al*., unpublished data). To increase the binding affinity and optimize the pharmacokinetic properties, a bivalent form of nanobody molecule was created by fusing two monovalent

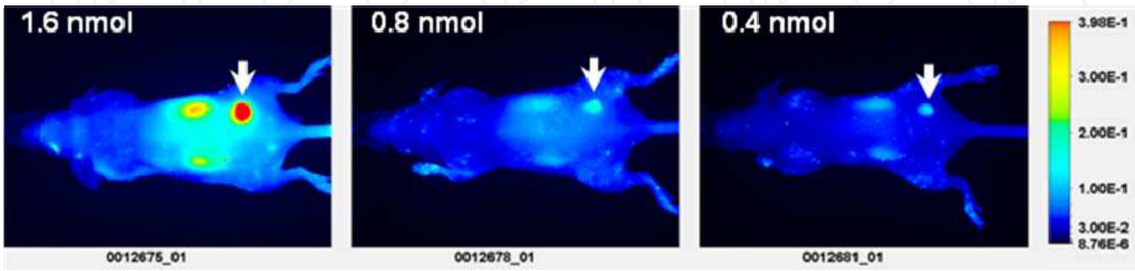

Fig. 1. *In vivo* fluorescence imaging of nude mice bearing A431 tumors using an EGFR-specific nanobody labeled with IRDye 800CW. Images (dorsal view) were acquired at 1 d after injection of 1.6 nmol, 0.8 nmol or 0.4 nmol imaging agents, respectively. Arrows indicate A431 tumors. The nanobody was a gift from Dr. Paul van Bergen en Henegouwen, Utrecht University.

nanobody (EG_2) molecules to the human Fc fragment. The resulting molecule, EG_2-hFc (80 kDa) was labeled with the fluorescent dye Cy5.5, and compared with Cy5.5-labeled monovalent EG_2, and Cy5.5-labeled pentavalent derivative V2C- EG_2 (128 kDa). *In vivo* pharmacokinetic and biodistribution studies in mice revealed that the plasma half life of EG_2-hFc-Cy5.5 was much prolonged compared to the other two probes. The retention of EG_2-hFc-Cy5.5 in EGFR/EGFRvIII-expressing orthotopic brain tumors was also significantly higher, resulting in an improved tumor fluorescence signal (Iqbal et al., 2010).

2.3 Natural ligand EGF

EGF (MW: 6045 Da) is a small polypeptide that binds with high affinity to EGFR on the cell surface (Stoscheck & King, 1986; Yarden & Sliwkowski, 2001). ^{111}In ($t_{1/2}$ = 2.8 d)-labeled hEGF (^{111}In-DTPA-hEGF) was compared with an ^{111}In-labeled monoclonal antibody (^{111}In-DTPA-MAb528) for *in vivo* tumor imaging. The blood clearance of ^{111}In-DTPA-hEGF was much faster (< 0.2%ID/g for ^{111}In-DTPA-hEGF *vs* 3%ID/g for ^{111}In-DTPA-MAb528 in the blood at 72 h post injection). The tumor accumulation of ^{111}In-DTPA-hEGF was lower. Although both probes could visualize EGFR-expressing tumors, the signal from ^{111}In-DTPA-MAb528 was more prominent at 72 h post-injection (Reilly et al., 2000). The fast clearance of EGF makes it advantageous over antibodies for radionuclides with shorter half-lives such as ^{68}Ga ($t_{1/2}$ = 68 min). ^{68}Ga-labeled hEGF (^{68}Ga-DOTA-hEGF) was used in a microPET imaging study. A quick localization of radioactivity in tumors (within 5 min) was demonstrated (Velikyan et al., 2005).

Both Cy5.5- and IRDye 800CW-labeled EGF (named as EGF-Cy5.5 and EGF800 respectively) have been successfully used for fluorescence optical imaging of EGFR-expressing tumors. The specificity of both probes was verified by competition with excess cetuximab (Ke et al., 2003; Kovar et al., 2006). However, a direct comparison between these two probes revealed that EGF800 produced a significantly lower background and a higher tumor-to-background ratio, implying that IRDye 800CW is superior to Cy5.5 for this application (Adams et al., 2007). Analysis of the excised tumors from EGF800-treated mice demonstrated a good correlation between tumor wet weight and *in vivo* tumor fluorescence signal. Repeated administration of EGF800 probe allowed for the non-invasive tracking of orthotopic prostate tumor growth (Fig. 2) (Kovar et al., 2006). Another study with EGF800 showed that probe accumulation in tumors reflected relative EGFR expression and EGFR occupancy by cetuximab (Manning et al., 2008).

QDs have also been used to label EGF for fluorescence optical imaging. An EGFR targeting nanoprobe was formed by coupling NIR QDs to EGF. The tumor-specific accumulation of this nanoprobe was demonstrated by both whole animal imaging and *ex vivo* tissue analysis (Diagaradjane et al., 2008).

2.4 EGFR-specific affibody

Affibody molecules are a class of affinity proteins composed of 58 amino acid residues that are derived from one of the IgG-binding domains of staphylococcal protein A. EGFR-specific affibody molecules (~7 kDa) have been selected by phage display technology (Friedman et al., 2007). A head-to-tail dimeric form $(Z_{EGFR:955})_2$ that has a higher binding affinity was labeled with ^{111}In and successfully used for *in vivo* imaging of A431 tumors

(Nordberg et al., 2008). To further improve the binding affinity and specificity, the affibody was optimized by affinity maturation process (Friedman et al., 2008). The second generation of EGFR-specific affibody has been conjugated with various labels, and characterized in detail.

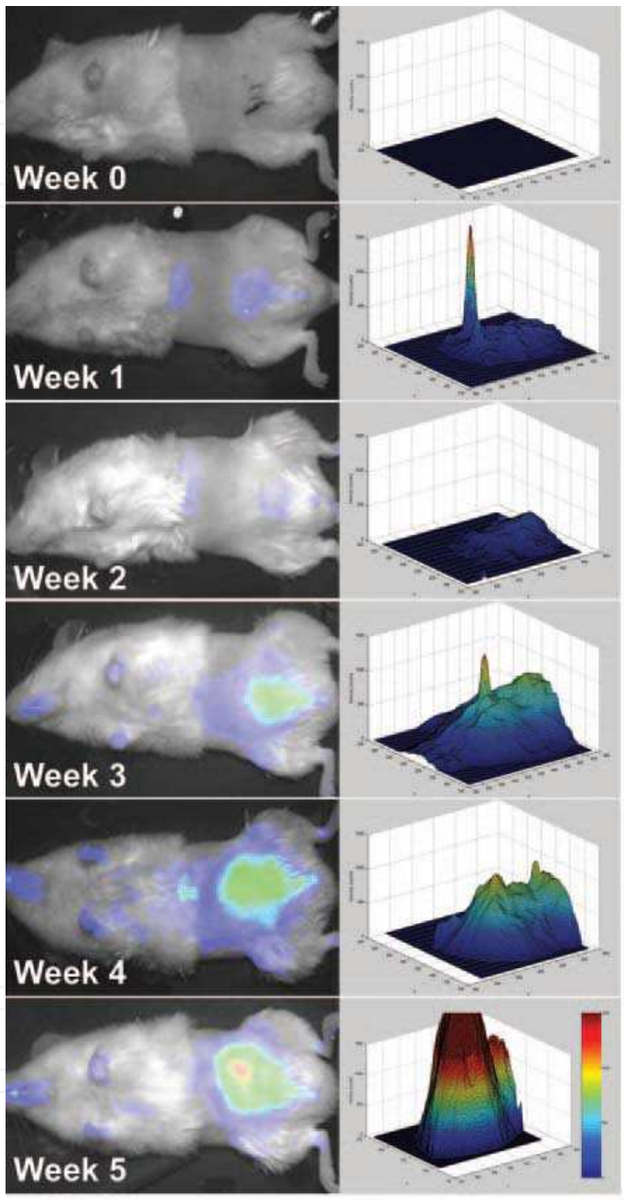

Fig. 2. Tracking of orthotopic prostate tumor growth with EGF800. Male NOD/SCID mice were injected orthotopically with 22Rv1 tumor cells. Animals were injected with EGF800 at different time points and imaged. The left column shows the tumor progression of a representative mouse in color-coded fluorescence images superimposed on the white light images. In the right column, total fluorescence in an ROI encompassing the tumor region was quantified. Fluorescence intensity is color-coded to assist visualization. Adapted from (Kovar et al., 2006) with permission.

In vivo imaging with ^{64}Cu- or Cy5.5-labeled $Z_{EGFR:1907}$ showed fast tumor (A431) targeting and good tumor-to-normal tissue contrast. Both agents accumulated at a high level in tumor, liver and kidney as revealed by biodistribution study (Miao et al., 2010, 2010). A dimeric form of EGFR-specific affibody (13.7 kDa) was labeled with IRDye 800CW (named as Eaff800), and used to image A431 xenograft tumors. The tumor could be visualized 1 h post-injection, and it became most prominent after 1 d (Fig. 3). The binding and uptake of Eaff800 was EGFR-specific because it only produced minimal signal when reacted with SK-OV-3 cells (HER2-overexpressing) in both cell-based assay and *in vivo* imaging study. It is notable that the liver uptake of Eaff800 was high, possibly due to the cross-reaction between Eaff800 and murine EGFR expressed in the liver (Gong et al., 2010).

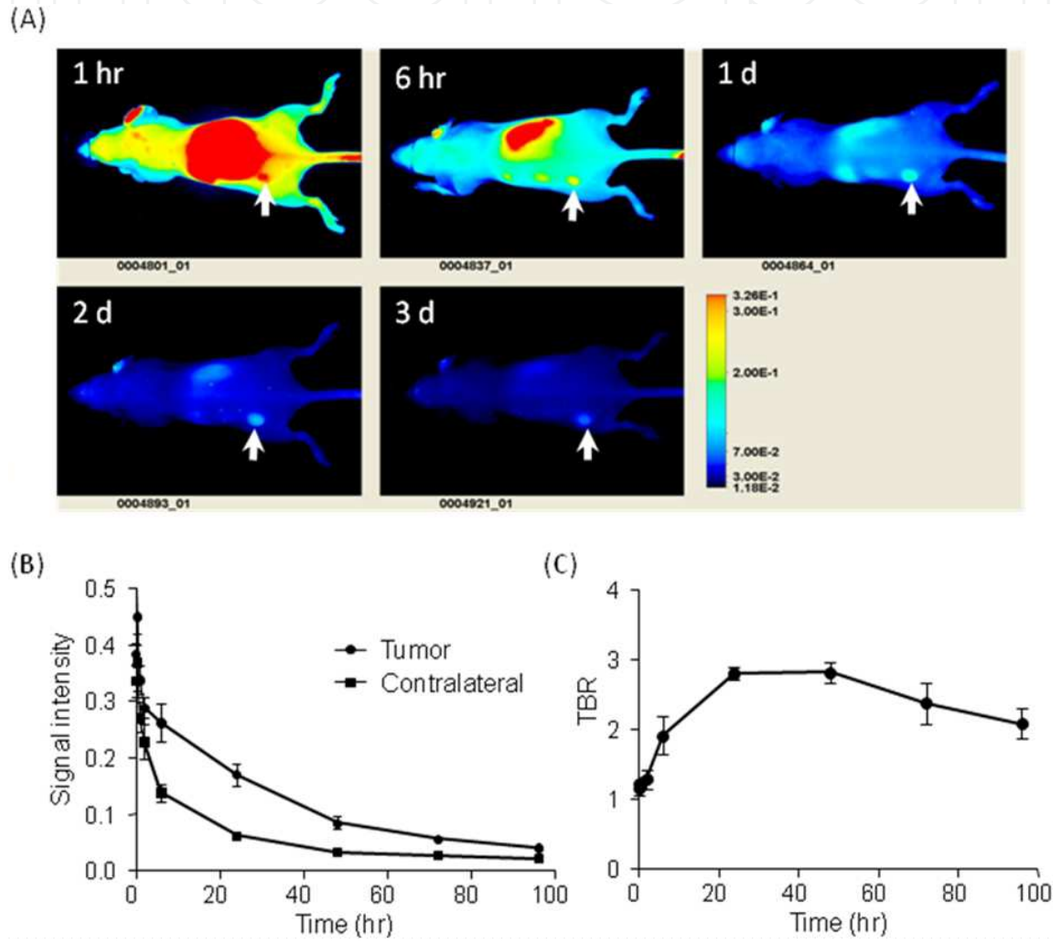

Fig. 3. *In vivo* optical imaging of nude mice bearing A431 tumors using Eaff800. (A) A representative series of whole body images (dorsal view) acquired at different time points following injection of 0.5 nmol Eaff800. The tumors were indicated with arrows. (B) Clearance of Eaff800 from the tumor and normal tissue. Average signal intensities were quantified using ROIs of equivalent sized areas from the tumor sites and contralateral sites at indicated time points. Data were presented as mean ± SD of three individual mice. (C) Tumor-to-background ratio (TBR) at different time points after probe injection. TBR was calculated by dividing mean tumor signal by mean background signal of the contralateral site. Adapted from (Gong et al., 2010) with permission.

The monomer $Z_{EGFR:1907}$ and dimer $(Z_{EGFR:1907})_2$ were labeled with ^{111}In and ^{125}I, respectively. The resulting four variants, ^{111}In-Bz-DTPA-$Z_{EGFR:1907}$, ^{111}In-Bz-DTPA-$(Z_{EGFR:1907})_2$, ^{125}I-PIB-$Z_{EGFR:1907}$ and ^{125}I-PIB-$(Z_{EGFR:1907})_2$ were compared in A431 tumor bearing nude mice. At 24 h after injection, the use of ^{111}In provided higher tumor radioactivity level than did ^{125}I for both the monomer and the dimer. It was also discovered that the tumor uptake of monomer was higher than that of dimer, despite a superior cellular retention of radioactivity for dimer in cell-based assays. The best probe, ^{111}In-Bz-DTPA-$Z_{EGFR:1907}$, produced a tumor-to-blood ratio of 100 at 24 h after injection (Tolmachev et al., 2009). To investigate the effect of injected protein dose, an aliquot of labeled affibody ^{111}In-DOTA-$Z_{EGFR:2377}$ was diluted in different amounts of unlabeled affibody before injection to A431 tumor bearing mice. A bell-shaped dose-responsive curve was observed. The initial increase in uptake was reasoned to be associated with saturation of EGFR in normal tissues, resulting in more ^{111}In-DOTA-$Z_{EGFR:2377}$ available for tumor targeting. Further increase in the unlabeled affibody caused the competition of EGFR in the tumor site and reduced ^{111}In-DOTA-$Z_{EGFR:2377}$ uptake (Tolmachev et al., 2010).

2.5 TKI derivatives

TKIs targeting EGFR are small organic molecules developed based mainly on the anilinoquinazoline moiety. These molecules bind to ATP-binding site of the kinase domain either reversibly or irreversibly (Mishani & Hagooly, 2009). Reversible TKI agent gefitinib was labeled with ^{18}F ($t_{1/2}$ = 110 min) to image the EGFR status of different cancer cells. However it was discovered that [^{18}F]-gefitinib uptake did not correlate with EGFR expression levels due to high non-specific cellular uptake (Su et al., 2008). This finding is in agreement with other studies showing that most reversible TKIs were inadequate for *in vivo* imaging despite impressive *in vitro* profile, including high affinity and specificity toward EGFR. These radio-labeled reversible agents often exhibit low uptake in targeted tumors and high uptake in non-targeted tissues (Mishani & Hagooly, 2009). Nevertheless, a recent study with ^{11}C ($t_{1/2}$ = 20 min)-labeled erlotinib, another reversible TKI, showed that [^{11}C]-erlotinib accumulated in HCC827 tumors that expresses high level of EGFR and is sensitive to erlotinib treatment. HCC827 xenograft tumors could be visualized by micro-PET scanning with [^{11}C]-erlotinib, whereas A549 and NCI358 xenografts (both express low level of EGFR) could not. However HCC827 cells also harbor an in-frame deletion mutation in exon 19 that contributes to the enhanced sensitivity to erlotinib. It is not clear whether this mutation causes the accumulation of [^{11}C]-erlotinib in the tumor (Memon et al., 2009).

To enhance binding efficacy, much effort has been invested in the development of irreversible TKIs as therapeutic drugs and imaging agents (Mishani et al., 2008; Mishani & Hagooly, 2009). An irreversible TKI-based radiotracer, morpholino-[^{124}I]-IPQA, has been developed and characterized. Morpholino-[^{124}I]-IPQA covalently binds to the ATP-binding site of the activated (phosphorylated) EGFR, but not the inactive EGFR. A431 tumors on immunocompromised rats and mice were successfully visualized by PET imaging with this probe (Pal et al., 2006). A newer version of this probe, [^{18}F]F-PEG6-IPQA, which has better water solubility, has also been developed. [^{18}F]F-PEG6-IPQA could detect NSCLC xenograft tumors harboring L858R activating EGFR mutations, and did not recognize NSCLC xenografts expressing either wild type or L858R/T790M dual mutant EGFR (Yeh et al., 2011). Another irreversible TKI analog ML04 exhibited excellent specificity to EGFR *in vitro*.

However, *in vivo* biodistribution analysis of [^{18}F]ML04 showed that the probe uptake in EGFR-positive tumors was mainly non-specific, suggesting that further optimization of this probe is needed (Abourbeh et al., 2007; Mishani et al., 2008).

3 Imaging HER2-overexpressing tumors

3.1 Anti-HER2 antibodies

HER2 amplification was initially observed in human breast cancer and was subsequently identified in ovarian cancer and other types of cancers (Niu et al., 2008; Slamon et al., 1989; Zhang et al., 1989). HER2 expression is highly conserved between primary breast lesions and metastases in lymph node, bone marrow as well as distant locations (Gancberg et al., 2002; Lopez-Guerrero et al., 2006; Regitnig et al., 2004; Simmons et al., 2009; Simon et al., 2001; Tapia et al., 2007; Vincent-Salomon et al., 2007); and remains so throughout therapy (Carlsson et al., 2004; Gong et al., 2005; Pectasides et al., 2006). Thus, accurate assessment of HER2 expression levels is of great interest for identifying breast cancer patients who will benefit from HER2-targeted therapy.

Trastuzumab (Herceptin; Genentech, CA), a recombinant humanized monoclonal antibody directed against the extracellular domain of the HER2 protein, was engineered by inserting the complementarity determining region of a murine antibody (clone 4D5) into the framework of a consensus human IgG1 (Carter et al., 1992). Tratuzumab has been shown to be effective in early-stage breast cancer that overexpresses HER2. Clinical trials indicate that combining tratuzumab treatment with standard chemotherapy for early-stage HER2 positive breast cancer reduces the risk of recurrence and death when compared to chemotherapy alone, thereby improving disease-free and overall survival rates in patients (Baselga et al., 2006; Romond et al., 2005).

Trastuzumab was radio-labeled with ^{111}In using DTPA as a chelator. ^{111}In-DTPA-trastuzumab selectively bound to the human HER2 receptor in *in vitro* analysis. Biodistribution and tumor targeting were studied in SK-OV-3 (HER2+) and GLC4 (HER2-) tumor-bearing athymic mice. The SK-OV-3 tumor showed substantial uptake of the labeled antibody after 5 h. The difference in uptake between SK-OV-3 and GLC4 tumors was even more pronounced 3 d after injection. At that time, the SK-OV-3 tumor was clearly visualized by radioimmunoscintigraphy (Lub-de Hooge et al., 2004). Research has also demonstrated that fluorescent dye-labeled trastuzumab enabled differentiation between breast cancer cells expressing high and low levels of HER2. Serial imaging before and during trastuzumab therapy revealed a significant reduction in probe uptake with treatment (Gee et al., 2008). Trastuzumab was also used to mediate the cellular internalization of pH-activatable fluorephores. These probes produced minimal fluorescence outside of the cell, and were activated by sensing the pH change in the lysosome after internalization (Urano et al., 2009). Other optical imaging based applications include imaging SK-BR-3 tumors with Cy5.5-labeled trastuzumab (Hilger et al., 2004), and distinguishing between HER2+ pulmonary metastases and HER2- pulmonary metastases using rhodamine green-conjugated trastuzumab (Koyama et al., 2007).

Another antibody against HER2 used for imaging applications is pertuzumab, a humanized antibody derived from the murine antibody 2C4. Unlike trastuzumab, pertuzumab sterically

hinders HER2 hetero-dimerization with EGFR and HER3. Pertuzumab conjugated with ^{177}Lu showed significant tumor uptake in an *in vivo* study using gamma camera imaging (Persson et al., 2005).

3.2 HER2-specific antibody fragments

Trastuzumab-derived antibody fragments Fab and F(ab')$_2$ have also been employed for molecular imaging. ^{111}In- or ^{99m}Tc-labeled trastuzumab Fab conjugates were used to detect HER2-expressing tumors using whole-body scintigraphy. Tumors were visualized 6 h post-injection (Tang et al., 2005; Tang et al., 2005). Trastuzumab and trastuzumab-derived Fab fragment (Fab4D5) labeled with ^{111}In were compared in a MMTV/HER2 mouse allograft model. Although Fab4D5 showed accumulation in the tumor as early as 2 h, rapid wash-out through the kidneys was observed by 6 h. On the contrary, trastuzumab was slow for tumor deposition and slow for clearance from the normal tissues. To improve the pharmacokinetic properties of the Fab fragment, an albumin binding sequence was introduced to generate a bifunctional molecule (AB.Fab4D5). Similar to Fab4D5 alone, AB.Fab4D5 visualized the tumor at 2 h post-injection, but its presence was sustained beyond 24 h, which resembles trastuzumab. Intravital microscopy revealed that tumor cell staining by AB.Fab4D5 was more uniform than for Fab4D5 or trastuzumab. The association of AB.Fab4D5 with albumin altered the clearance route of the probe, and minimal probe accumulation in the kidney was observed (Dennis et al., 2007). In another report, trastuzumab F(ab')$_2$ fragment labeled with ^{68}Ga was successfully used to quantify the loss and recovery of HER2 induced by HSP90 inhibitor 17-AAG in mice bearing BT-474 tumors (Smith-Jones et al., 2004). Table 1 summarizes trastuzumab-based agents for nuclear, optical and dual-modality imaging. This table includes only representative agents in each class, thus is in no way a complete list. The dual-labeled probes listed here will be discussed in detail later.

Imaging modality	Imaging agents	Animal model and cell lines	Dosage	Reference
Nuclear medicine				
PET	^{64}Cu-DOTA-Herceptin, ^{68}Ga-DOTA-F(ab')$_2$	Mouse xenograft; BT-474, MCF-7, MDA-MB-468	4 MBq 309 MBq	(Smith-Jones et al., 2004)
	^{89}Zr-trastuzumab	Mouse xenograft; SKOV3, GLC4	100 µg of trastuzumab (1 MBq)	(Dijkers et al., 2009)
SPECT/CT	^{111}In-DOTA-Fab4D5, ^{111}In-DOTA-AB.Fab4D5	Mouse allograft; tumors derived from MMTV/HER2 transgenic mice	4 mg/kg (300-500 µCi)	(Dennis et al., 2007)

Scintigraphy (whole body)	[^{99m}Tc]-HYNIC-trastuzumab Fab, ^{111}In-trastuzumab Fab, ^{111}In-DTPA-trastuzumab	Mouse xenograft; BT-474, SK-OV-3 human	25 MBq (30μg) 3.7 MBq (30μg) Mice: 450 ± 25 kBq (25 μg); Human: 100-150 MBq (5mg)	(Lub-de Hooge et al., 2004; Tang et al., 2005; Tang et al., 2005)
Optical imaging				
Fluorescent dyes	Herceptin-RhodG	Mouse xenograft; SK-BR-3, PE/CA-PJ34	50 μg in 200 μl PBS	(Koyama et al., 2007)
	Tra-Cy5.5 (SQ), Tra-Alexa680(SQ)	Mouse xenograft; 3T3/HER2+, Balb/3T3/HER2-	50 μg/100 μL PBS	(Ogawa et al., 2009)
	Trastuzumab-Cy5.5, Trastuzumab-AF750	Mouse xenograft; 9L, MCF-7, BT-474, SK-BR-3	0.4 nmol	(Gee et al., 2008)
Quantum dots (QDs)	Trastuzumab-QD	Mouse xenograft; 3T3/HER2+, Balb/3T3/HER2-	2 μM (100 μl)	(Li-Shishido et al., 2006; Tada et al., 2007)
Dual-modality				
Nuclear and optical agents	(^{111}In-DTPA)$_n$-trastuzumab-(IRDye800)$_m$	Mouse xenograft; SKBr3-luc	80-200 μg (70-200 μCi)	(Sampath et al., 2007)
	(^{64}Cu-DOTA)$_n$-trastuzumab-(IRDye800)$_m$	Mouse allograft; 4T1.2/R, 4T1.2neu/R	150 μg (150 μCi)	(Sampath et al., 2010)
	^{111}In-trastuzumab-ICG	Mouse xenograft; 3T3/HER2, MDA-MB-468	60 μg (3.8 MBq)	(Ogawa et al., 2009)

Table 1. Summary of molecular imaging agents based on trastuzumab (Herceptin) or trastuzumab fragments

3.3 HER2-specific affibody

Phage display selection yielded affibody molecules that specifically bind to HER2 extracellular domain. One of these molecules, His_6-$Z_{HER2:4}$ (affibody $Z_{HER2:4}$ linked to a histidine tag) targets the extracellular domain of HER2 with an affinity (K_D) at about 50 nM. The affibody does not interfere with trastuzumab binding to HER2, since the binding sites are different (Wikman et al., 2004). The specificity of the affibody was illustrated by the uptake of ^{125}I- His_6-$Z_{HER2:4}$ in HER2-overexpressing SK-BR-3 breast cancer cells (Tran et al., 2007; Wikman et al., 2004). A bivalent version of the affibody $(Z_{HER2:4})_2$, which has an increased binding affinity (K_D = 3 nM) was later created (Steffen et al., 2005). When ^{125}I-labeled $(Z_{HER2:4})_2$ was investigated in an animal study, a tumor-to-blood ratio of about 10:1 was obtained 8 h after injection, and the tumor region could be visualized using gamma camera imaging (Steffen et al., 2006). However a comparison of ^{125}I-labeled (Tolmachev et al., 2009) or ^{18}F-labeled (Cheng et al., 2008) second generation affibody molecules (see below) demonstrated that the monomeric form provided better tumor targeting than the dimeric form, which is the same as EGFR-specific affibody molecules (Tolmachev et al., 2009).

The second generation of HER2-specific affibody was generated through a single-library affinity maturation step. One of them, $Z_{HER2:342}$, showed a >2200-fold increase in affinity (22 pM for $Z_{HER2:342}$ *vs* 50 nM for $Z_{HER2:4}$). SK-OV-3 tumor xenografts were imaged 6 h after injection of ^{125}I-labeled $Z_{HER2:342}$. The tumor uptake at 4 h post-injection was improved by a factor of 4 compared to the parental molecule $Z_{HER2:4}$ (Orlova et al., 2006). Comparison of ^{124}I-labeled $Z_{HER2:342}$ and trastuzumab demonstrated that better tumor-to-organ ratios were obtained with $Z_{HER2:342}$ due to the more rapid clearance (Orlova et al., 2009). By changing the radioisotope to ^{111}In, the labeled molecule ^{111}In-Benzyl-DTPA- $Z_{HER2:342}$ maintain a K_D of 21 pM. Detection of SK-OV-3 tumors was achieved at 4 h post-injection with a gamma-camera. Biodistribution analysis revealed a tumor-to-blood ratio of 100 (Tolmachev et al., 2006). HER2-specific affibody molecules were also labeled with fluorescent dyes. The binding affinities and specificities of the conjugated molecules were unchanged or minimally affected by the modifications. *In vivo* NIR optical imaging revealed that affibody fused with an albumin-binding domain (ABD-$(Z_{HER2:342})_2$) exhibited a better performance compared to either monomer or dimer alone (Lee et al., 2008).

Site-specific radio-labeling of $Z_{HER2:342}$ was achieved by synthetic chemistry. The resulting ^{111}In-DOTA-$Z_{HER2:342\text{-}pep2}$ has a binding affinity of 65 pM. High contrast gamma camera images were obtained in the tumor region as early as 1 h after injection. Although pre-treatment with trastuzumab did not compete with the binding of ^{111}In-DOTA-$Z_{HER2:342\text{-}pep2}$ in tumors, degradation of the HER2 receptor using the heat-shock 90 inhibitor 17-AAG before probe administration reduced tumor uptake (Orlova et al., 2007). These data taken together indicate that, similar to the first generation affibody $Z_{HER2:4}$, the binding site of $Z_{HER2:342}$ is different from that of trastuzumab, but specific to the HER2 receptor. Site-specific labeling of ^{99m}Tc was mediated by incorporation of either histidine tag (His_6), natural peptide sequences CCG, CGGG, or maGGG, maSSS, maSKS, maESE chelators into the $Z_{HER2:342}$ sequence. All ^{99m}Tc-labeled probes showed tumor-specific uptake at 6 h post-injection or earlier using gamma camera imaging (Engfeldt et al., 2007; Engfeldt et al., 2007; Orlova et al., 2006; Tran et al., 2007; Tran et al., 2008).

^{111}In and ^{68}Ga-labeled $Z_{HER2:342}$ were tested in patients with recurrent metastatic breast cancer. These agents detected 9 out of 11 ^{18}F-FDG-positive metastases at 2-3 h after injection,

suggesting their potential to localize HER2-positive metastases not amenable to biopsy (Baum et al., 2010).

The HER2-specific affibody was further optimized by reengineering the nonbinding surface of $Z_{HER2:342}$ to improve its properties such as storage stability, surface hydrophilicity, melting point and amenability for peptide synthesis. The new generation of affibody was created and characterized (Ahlgren et al., 2010; Feldwisch et al., 2010).

The fact that HER2-specific affibodies and trastuzumab target separate epitopes might be advantageous when developing these affibodies as imaging agents. These imaging agents will not interfere with trastuzumab binding when being used to monitor the therapeutic effect of trastuzumab (Baum et al., 2010; Orlova et al., 2007). One cause of concern of these affibody-base imaging agents is the high non-specific kidney accumulation. This is due to the small molecular weight of the affibody molecules which renders their clearance mainly through the kidney.

3.4 Dual-labeled trastuzumab

Probes dual-labeled with a radionuclide and a NIR fluorophore enhance the advantages and compensate the disadvantages of each modality, and could offer unique opportunities for the combination of non-invasive whole body imaging and subsequent intraoperative guidance during surgery. To investigate this possibility, trastuzumab was conjugated with either ^{111}In (for SPECT imaging) or ^{64}Cu (for PET imaging), and IRDye 800CW to image HER2 overexpression in mouse xenograft tumors (Sampath et al., 2010; Sampath et al., 2007).

(^{111}In-DTPA)$_n$-trastuzumab-(IRDye800)$_m$ was synthesized using a three step process wherein, trastuzumab was first conjugated to DTPA and then with IRDye 800CW. Prior to animal imaging, radio-labeling with ^{111}In was performed. The agent was validated for binding specificity *in vitro* using the fluorescence microscopy. High probe uptake in HER2-overexpressing SKBr3-luc tumors was demonstrated using NIR fluorescence, SPECT and planar scintigraphy imaging. The tumor-to-muscle ratios were comparable between optical and nuclear imaging modalities, but NIR fluorescence imaging had a higher signal-to-noise ratio. Since NIR fluorescence imaging has improved sensitivity due to high photon count, it can be used to monitor the lymphatic uptake of the dual-labeled antibody after intradermal administration into the dorsal aspect of the foot pad. Accumulation into the lymph nodes was observed at picomole doses within 1 h after administration, while clearance was observed by 24 h (Sampath et al., 2007).

To test the ability of dual-labeled (^{64}Cu-DOTA)$_n$-trastuzumab-(IRDye800)$_m$ to detect metastasis, Balb/c mice bearing 4T1.2/R (murine breast cancer cell, HER-) and 4T1.2neu/R (murine breast cancer cell, HER+) tumors were used. The diagnostic capability of this dual-labeled probe was also compared with PET imaging agent ^{18}FDG. (^{64}Cu-DOTA)$_n$-trastuzumab-(IRDye800)$_m$ showed significantly higher uptake in 4T1.2neu/R primary tumors compared to 4T1.2/R tumors, indicating *in vivo* specificity of the dual-labeled imaging agent. In contrast ^{18}FDG did not show any preferential uptake between the two tumor types. Lung metastases of HER2-overexpressing 4T1.2neu/R cells were successfully detected with whole body PET imaging after administration of (^{64}Cu-DOTA)$_n$-trastuzumab-

$(IRDye800)_m$. Unfortunately, due to its limited penetration capability, whole body NIR fluorescence imaging could not detect lung metastases although it detected superficial skin metastases successfully. But agent uptake was evident with *ex vivo* NIR fluorescence imaging. *Ex vivo* NIR fluorescence imaging also visualized the trafficking of imaging agent from the primary tumor to lymph nodes, which was not possible for nuclear imaging with ^{64}Cu. When ^{18}FDG was investigated, it could not detect metastases under these conditions (Sampath et al., 2010).

In another study, it was found that trastuzumab labeled with both ICG and ^{111}In mimicked the cocktail of ICG-trastuzumab and ^{111}In-trastuzumab when injected into 3T3/HER2 tumor-bearing mice. As the fluorescence of ICG in this probe was only activated after binding to the HER2 receptor on the cell surface and being internalized, the HER2-overexpressing tumor could be visualized with minimal background signal (Ogawa et al., 2009).

4 Imaging EGFR and HER2 simultaneously

4.1 Antibodies labeled with fluorescent dyes

Fluorescence optical imaging has the advantage of multiple channels, which can be employed to image two or more targets simultaneously. Cetuximab and trastuzumab were labeled with Cy5.5 and Cy7, respectively. The binding and internalization of cetuximab-Cy5.5 by A431, and trastuzumab-Cy7 by 3T3/HER2+ cells were confirmed by fluorescence microscopy. On the contrary, no binding of cetuximab-Cy5.5 to 3T3/HER2+, and trastuzumab-Cy7 to A431 was observed. When mice were injected with a cocktail of cetuximab-Cy5.5 and trastuzumab-Cy7, A431 and 3T3/HER2+ tumors could be detected distinctly based on the Cy5.5 and Cy7 spectral images (Barrett et al., 2007). In a subsequent study three antibodies (cetuximab, trastuzumab and daclizumab) were labeled with three different fluorophores (Cy5, Cy7 and AlexaFluor700), respectively. Spectrally resolved fluorescence imaging showed that these probes clearly distinguished their respective targeting tumors (A431, 3T3/HER2+ and SP2-Tac) based on their distinct optical spectra (Koyama et al., 2007).

4.2 Affibody molecules labeled with fluorescent dyes

The EGFR- or HER2-specific Affibody molecules were labeled with IRDye 800CW and DY-682, respectively. The labeled probes, Eaff800 and Haff682, were taken up at high levels by EGFR-overexpressing A431 and HER2-overexpressing SK-OV-3 cells, respectively. Whole animal imaging showed that Eaff800 mainly accumulated in A431 tumor, while more Haff682 signal was found in SK-OV-3 tumor (Fig. 4A). Scanning tissue sections of dissected tumors confirmed the *in vivo* data. The liver uptake of Eaff800 was much higher than that of Haff682, suggesting a role of murine liver EGFR in the uptake of Eaff800. When the labeled fluorophores on the affibody molecules were exchanged (i.e. EGFR-specific affibody labeled with DY-682 and HER-specific affibody labeled with IRDye 800CW), the specificities of the affibody molecules were not affected (Fig. 4B). These results demonstrated that the tumor uptake of these imaging agents is receptor-mediated, and is independent of the fluorophore labeled on the affibody molecules (Gong et al., 2010).

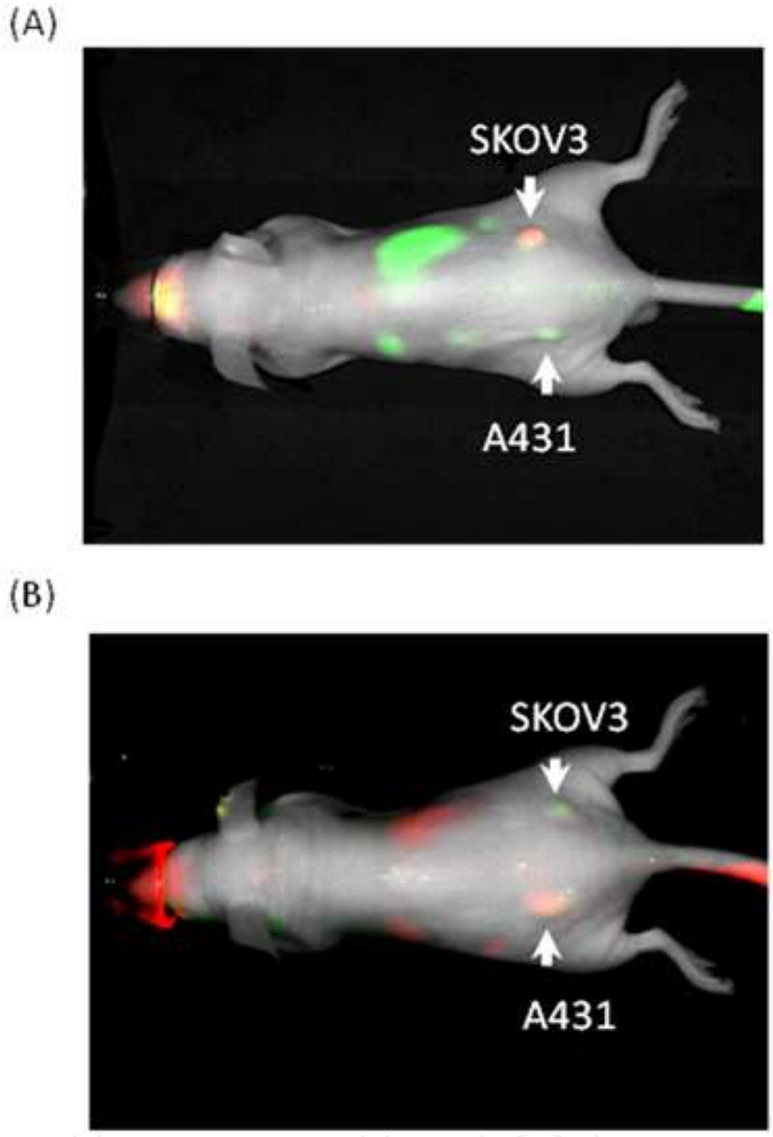

Fig. 4. Dual-color *in vivo* optical imaging with EGFR- and HER2-specific affibody molecules. Nude mice bearing A431 and SK-OV-3 tumors on the left side and right side, respectively, were injected with 100 µl PBS containing (A) 0.5 nmol Eaff800 and 0.5 nmol Haff682, or (B) 0.5 nmol Haff800 and 0.5 nmol Eaff682. Whole body images (dorsal view) were acquired at 1d following agent injection. The green color and red color represent IRDye800CW and DY-682 fluorescence signals, respectively. The tumors were indicated with arrows. Modified from (Gong et al., 2010) with permission.

5. Closing remarks

In vivo molecular imaging has become a valuable tool in biomedical research and drug development (Weissleder & Pittet, 2008; Willmann et al., 2008). The radionuclide-based imaging technology, such as PET and SPECT, has been used in clinical applications. In the research field, fluorescence optical imaging is becoming more and more popular due to its

low cost, ease of use, longer time window for image capture and ability to track multiple probes simultaneously. Compared to fluorophores in the visible spectra, imaging with NIR fluorophores could reduce the autofluorescence, maximize tissue penetration, and are ideally suitable for non-invasive animal imaging applications (Kovar et al., 2007; Weissleder, 2001). However, even with NIR fluorophores, the direct clinical application of fluorescence imaging may be limited to superficial tissues such as breast and skin, or for visualization during endoscopy and image-guided-surgery procedures (Kampmeier et al., 2010).

EGFR- and HER2-targeted molecular imaging may aid in the selection of patients for individualized therapy by noninvasively assessing the expression level of EGFR and HER2 in tumors, and guide drug dosage and regime by measuring target-drug interaction and receptor occupancy. It can also be used to assess the responses to therapy in pre-clinical and clinical research, and provide valuable information for drug development and validation (Kampmeier et al., 2010).

EGFR and HER2 mediate a complex network of signaling pathways that interweaves with many other signaling networks. Interpretation of therapeutic output based solely on EGFR- and HER2-targeted imaging results might be oversimplified. Analysis of downstream molecules such as p-Erk1/2 may complement EGFR- and HER2-targeted imaging and provide new insights for cancer treatment (Cai et al., 2008). For EGFR-targeted therapy, it is not uncommon that drug effects are independent of EGFR expression levels in cancer cells. In these situations, targeting activated forms of the receptor instead of total receptor level may be a more reliable method to predict drug responsiveness (Pantaleo et al., 2009; Pantaleo et al., 2009).

6. References

Abourbeh G, Dissoki S, Jacobson O, Litchi A, Ben Daniel R, Laki D, Levitzki A & Mishani E (2007) Evaluation of radiolabeled ML04, a putative irreversible inhibitor of epidermal growth factor receptor, as a bioprobe for PET imaging of EGFR-overexpressing tumors. *Nucl Med Biol* 34: 55-70

Adams KE, Ke S, Kwon S, Liang F, Fan Z, Lu Y, Hirschi K, Mawad ME, Barry MA & Sevick-Muraca EM (2007) Comparison of visible and near-infrared wavelength-excitable fluorescent dyes for molecular imaging of cancer. *J Biomed Opt* 12: 024017

Ahlgren S, Orlova A, Wallberg H, Hansson M, Sandstrom M, Lewsley R, Wennborg A, Abrahmsen L, Tolmachev V & Feldwisch J (2010) Targeting of HER2-expressing tumors using 111In-ABY-025, a second-generation affibody molecule with a fundamentally reengineered scaffold. *J Nucl Med* 51: 1131-1138

Barrett T, Koyama Y, Hama Y, Ravizzini G, Shin IS, Jang BS, Paik CH, Urano Y, Choyke PL & Kobayashi H (2007) *In vivo* diagnosis of epidermal growth factor receptor expression using molecular imaging with a cocktail of optically labeled monoclonal antibodies. *Clin Cancer Res* 13: 6639-6648

Baselga J (2006) Targeting tyrosine kinases in cancer: the second wave. *Science* 312: 1175-1178

Baselga J, Perez EA, Pienkowski T & Bell R (2006) Adjuvant trastuzumab: a milestone in the treatment of HER-2-positive early breast cancer. *Oncologist* 11 Suppl 1: 4-12

Baum RP, Prasad V, Muller D, Schuchardt C, Orlova A, Wennborg A, Tolmachev V & Feldwisch J (2010) Molecular imaging of HER2-expressing malignant tumors in

breast cancer patients using synthetic 111In- or 68Ga-labeled affibody molecules. *J Nucl Med* 51: 892-897

Cai W, Chen K, He L, Cao Q, Koong A & Chen X (2007) Quantitative PET of EGFR expression in xenograft-bearing mice using 64Cu-labeled cetuximab, a chimeric anti-EGFR monoclonal antibody. *Eur J Nucl Med Mol Imaging* 34: 850-858

Cai W, Niu G & Chen X (2008) Multimodality imaging of the HER-kinase axis in cancer. *Eur J Nucl Med Mol Imaging* 35: 186-208

Carlsson J, Nordgren H, Sjostrom J, Wester K, Villman K, Bengtsson NO, Ostenstad B, Lundqvist H & Blomqvist C (2004) HER2 expression in breast cancer primary tumours and corresponding metastases. Original data and literature review. *Br J Cancer* 90: 2344-2348

Carter P, Presta L, Gorman CM, Ridgway JB, Henner D, Wong WL, Rowland AM, Kotts C, Carver ME & Shepard HM (1992) Humanization of an anti-p185HER2 antibody for human cancer therapy. *Proc Natl Acad Sci U S A* 89: 4285-4289

Cheng Z, De Jesus OP, Namavari M, De A, Levi J, Webster JM, Zhang R, Lee B, Syud FA & Gambhir SS (2008) Small-animal PET imaging of human epidermal growth factor receptor type 2 expression with site-specific 18F-labeled protein scaffold molecules. *J Nucl Med* 49: 804-813

Dennis MS, Jin H, Dugger D, Yang R, McFarland L, Ogasawara A, Williams S, Cole MJ, Ross S & Schwall R (2007) Imaging tumors with an albumin-binding Fab, a novel tumor-targeting agent. *Cancer Res* 67: 254-261

Diagaradjane P, Orenstein-Cardona JM, Colon-Casasnovas NE, Deorukhkar A, Shentu S, Kuno N, Schwartz DL, Gelovani JG & Krishnan S (2008) Imaging epidermal growth factor receptor expression *in vivo*: pharmacokinetic and biodistribution characterization of a bioconjugated quantum dot nanoprobe. *Clin Cancer Res* 14: 731-741

Dijkers EC, Kosterink JG, Rademaker AP, Perk LR, van Dongen GA, Bart J, de Jong JR, de Vries EG & Lub-de Hooge MN (2009) Development and characterization of clinical-grade 89Zr-trastuzumab for HER2/neu immunoPET imaging. *J Nucl Med* 50: 974-981

Ekstrand AJ, Sugawa N, James CD & Collins VP (1992) Amplified and rearranged epidermal growth factor receptor genes in human glioblastomas reveal deletions of sequences encoding portions of the N- and/or C-terminal tails. *Proc Natl Acad Sci U S A* 89: 4309-4313

Engfeldt T, Orlova A, Tran T, Bruskin A, Widstrom C, Karlstrom AE & Tolmachev V (2007) Imaging of HER2-expressing tumours using a synthetic Affibody molecule containing the 99mTc-chelating mercaptoacetyl-glycyl-glycyl-glycyl (MAG3) sequence. *Eur J Nucl Med Mol Imaging* 34: 722-733

Engfeldt T, Tran T, Orlova A, Widstrom C, Feldwisch J, Abrahmsen L, Wennborg A, Karlstrom AE & Tolmachev V (2007) 99mTc-chelator engineering to improve tumour targeting properties of a HER2-specific Affibody molecule. *Eur J Nucl Med Mol Imaging* 34: 1843-1853

Feldwisch J, Tolmachev V, Lendel C, Herne N, Sjoberg A, Larsson B, Rosik D, Lindqvist E, Fant G, Hoiden-Guthenberg I, Galli J, Jonasson P & Abrahmsen L (2010) Design of an optimized scaffold for affibody molecules. *J Mol Biol* 398: 232-247

Ferguson KM, Darling PJ, Mohan MJ, Macatee TL & Lemmon MA (2000) Extracellular domains drive homo- but not hetero-dimerization of erbB receptors. *EMBO J* 19: 4632-4643

Friedman M, Nordberg E, Hoiden-Guthenberg I, Brismar H, Adams GP, Nilsson FY, Carlsson J & Stahl S (2007) Phage display selection of Affibody molecules with specific binding to the extracellular domain of the epidermal growth factor receptor. *Protein Eng Des Sel* 20: 189-199

Friedman M, Orlova A, Johansson E, Eriksson TL, Hoiden-Guthenberg I, Tolmachev V, Nilsson FY & Stahl S (2008) Directed evolution to low nanomolar affinity of a tumor-targeting epidermal growth factor receptor-binding affibody molecule. *J Mol Biol* 376: 1388-1402

Gainkam LO, Huang L, Caveliers V, Keyaerts M, Hernot S, Vaneycken I, Vanhove C, Revets H, De Baetselier P & Lahoutte T (2008) Comparison of the biodistribution and tumor targeting of two 99mTc-labeled anti-EGFR nanobodies in mice, using pinhole SPECT/micro-CT. *J Nucl Med* 49: 788-795

Gancberg D, Di Leo A, Cardoso F, Rouas G, Pedrocchi M, Paesmans M, Verhest A, Bernard-Marty C, Piccart MJ & Larsimont D (2002) Comparison of HER-2 status between primary breast cancer and corresponding distant metastatic sites. *Ann Oncol* 13: 1036-1043

Gee MS, Upadhyay R, Bergquist H, Alencar H, Reynolds F, Maricevich M, Weissleder R, Josephson L & Mahmood U (2008) Human breast cancer tumor models: molecular imaging of drug susceptibility and dosing during HER2/neu-targeted therapy. *Radiology* 248: 925-935

Gong H, Kovar J, Little G, Chen H & Olive DM (2010) *In vivo* imaging of xenograft tumors using an epidermal growth factor receptor-specific affibody molecule labeled with a near-infrared fluorophore. *Neoplasia* 12: 139-149

Gong Y, Booser DJ & Sneige N (2005) Comparison of HER-2 status determined by fluorescence in situ hybridization in primary and metastatic breast carcinoma. *Cancer* 103: 1763-1769

Hama Y, Urano Y, Koyama Y, Choyke PL & Kobayashi H (2007) Activatable fluorescent molecular imaging of peritoneal metastases following pretargeting with a biotinylated monoclonal antibody. *Cancer Res* 67: 3809-3817

Hamers-Casterman C, Atarhouch T, Muyldermans S, Robinson G, Hamers C, Songa EB, Bendahman N & Hamers R (1993) Naturally occurring antibodies devoid of light chains. *Nature* 363: 446-448

Hilger I, Leistner Y, Berndt A, Fritsche C, Haas KM, Kosmehl H & Kaiser WA (2004) Near-infrared fluorescence imaging of HER-2 protein over-expression in tumour cells. *Eur Radiol* 14: 1124-1129

Holliger P & Hudson PJ (2005) Engineered antibody fragments and the rise of single domains. *Nat Biotechnol* 23: 1126-1136

Huang L, Gainkam LO, Caveliers V, Vanhove C, Keyaerts M, De Baetselier P, Bossuyt A, Revets H & Lahoutte T (2008) SPECT imaging with 99mTc-labeled EGFR-specific nanobody for *in vivo* monitoring of EGFR expression. *Mol Imaging Biol* 10: 167-175

Iqbal U, Trojahn U, Albaghdadi H, Zhang J, O'Connor-McCourt M, Stanimirovic D, Tomanek B, Sutherland G & Abulrob A (2010) Kinetic analysis of novel mono- and

multivalent VHH-fragments and their application for molecular imaging of brain tumours. *Br J Pharmacol* 160: 1016-1028

Kampmeier F, Niesen J, Koers A, Ribbert M, Brecht A, Fischer R, Kiessling F, Barth S & Thepen T (2010) Rapid optical imaging of EGF receptor expression with a single-chain antibody SNAP-tag fusion protein. *Eur J Nucl Med Mol Imaging* 37: 1926-1934

Kari C, Chan TO, Rocha de Quadros M & Rodeck U (2003) Targeting the epidermal growth factor receptor in cancer: apoptosis takes center stage. *Cancer Res* 63: 1-5

Ke S, Wen X, Gurfinkel M, Charnsangavej C, Wallace S, Sevick-Muraca EM & Li C (2003) Near-infrared optical imaging of epidermal growth factor receptor in breast cancer xenografts. *Cancer Res* 63: 7870-7875

Keppler A, Pick H, Arrivoli C, Vogel H & Johnsson K (2004) Labeling of fusion proteins with synthetic fluorophores in live cells. *Proc Natl Acad Sci U S A* 101: 9955-9959

Kovar JL, Johnson MA, Volcheck WM, Chen J & Simpson MA (2006) Hyaluronidase expression induces prostate tumor metastasis in an orthotopic mouse model. *Am J Pathol* 169: 1415-1426

Kovar JL, Simpson MA, Schutz-Geschwender A & Olive DM (2007) A systematic approach to the development of fluorescent contrast agents for optical imaging of mouse cancer models. *Anal Biochem* 367: 1-12

Koyama Y, Barrett T, Hama Y, Ravizzini G, Choyke PL & Kobayashi H (2007) *In vivo* molecular imaging to diagnose and subtype tumors through receptor-targeted optically labeled monoclonal antibodies. *Neoplasia* 9: 1021-1029

Koyama Y, Hama Y, Urano Y, Nguyen DM, Choyke PL & Kobayashi H (2007) Spectral fluorescence molecular imaging of lung metastases targeting HER2/neu. *Clin Cancer Res* 13: 2936-2945

Lang SA, Klein D, Moser C, Gaumann A, Glockzin G, Dahlke MH, Dietmaier W, Bolder U, Schlitt HJ, Geissler EK & Stoeltzing O (2007) Inhibition of heat shock protein 90 impairs epidermal growth factor-mediated signaling in gastric cancer cells and reduces tumor growth and vascularization *in vivo*. *Mol Cancer Ther* 6: 1123-1132

Lee FT, O'Keefe GJ, Gan HK, Mountain AJ, Jones GR, Saunder TH, Sagona J, Rigopoulos A, Smyth FE, Johns TG, Govindan SV, Goldenberg DM, Old LJ & Scott AM (2010) Immuno-PET quantitation of de2-7 epidermal growth factor receptor expression in glioma using 124I-IMP-R4-labeled antibody ch806. *J Nucl Med* 51: 967-972

Lee SB, Hassan M, Fisher R, Chertov O, Chernomordik V, Kramer-Marek G, Gandjbakhche A & Capala J (2008) Affibody molecules for *in vivo* characterization of HER2-positive tumors by near-infrared imaging. *Clin Cancer Res* 14: 3840-3849

Li-Shishido S, Watanabe TM, Tada H, Higuchi H & Ohuchi N (2006) Reduction in nonfluorescence state of quantum dots on an immunofluorescence staining. *Biochem Biophys Res Commun* 351: 7-13

Lopez-Guerrero JA, Llombart-Cussac A, Noguera R, Navarro S, Pellin A, Almenar S, Vazquez-Alvadalejo C & Llombart-Bosch A (2006) HER2 amplification in recurrent breast cancer following breast-conserving therapy correlates with distant metastasis and poor survival. *Int J Cancer* 118: 1743-1749

Lub-de Hooge MN, Kosterink JG, Perik PJ, Nijnuis H, Tran L, Bart J, Suurmeijer AJ, de Jong S, Jager PL & de Vries EG (2004) Preclinical characterisation of 111In-DTPA-trastuzumab. *Br J Pharmacol* 143: 99-106

Manning HC, Merchant NB, Foutch AC, Virostko JM, Wyatt SK, Shah C, McKinley ET, Xie J, Mutic NJ, Washington MK, LaFleur B, Tantawy MN, Peterson TE, Ansari MS, Baldwin RM, Rothenberg ML, Bornhop DJ, Gore JC & Coffey RJ (2008) Molecular imaging of therapeutic response to epidermal growth factor receptor blockade in colorectal cancer. *Clin Cancer Res* 14: 7413-7422

Memon AA, Jakobsen S, Dagnaes-Hansen F, Sorensen BS, Keiding S & Nexo E (2009) Positron emission tomography (PET) imaging with [11C]-labeled erlotinib: a micro-PET study on mice with lung tumor xenografts. *Cancer Res* 69: 873-878

Miao Z, Ren G, Liu H, Jiang L & Cheng Z (2010) Cy5.5-labeled Affibody molecule for near-infrared fluorescent optical imaging of epidermal growth factor receptor positive tumors. *J Biomed Opt* 15: 036007

Miao Z, Ren G, Liu H, Jiang L & Cheng Z (2010) Small-animal PET imaging of human epidermal growth factor receptor positive tumor with a 64Cu labeled affibody protein. *Bioconjug Chem* 21: 947-954

Mishani E, Abourbeh G, Eiblmaier M & Anderson CJ (2008) Imaging of EGFR and EGFR tyrosine kinase overexpression in tumors by nuclear medicine modalities. *Curr Pharm Des* 14: 2983-2998

Mishani E & Hagooly A (2009) Strategies for molecular imaging of epidermal growth factor receptor tyrosine kinase in cancer. *J Nucl Med* 50: 1199-1202

Mitsudomi T & Yatabe Y (2010) Epidermal growth factor receptor in relation to tumor development: EGFR gene and cancer. *FEBS J* 277: 301-308

Niu G, Cai W, Chen K & Chen X (2008) Non-invasive PET imaging of EGFR degradation induced by a heat shock protein 90 inhibitor. *Mol Imaging Biol* 10: 99-106

Niu G, Cai W & Chen X (2008) Molecular imaging of human epidermal growth factor receptor 2 (HER-2) expression. *Front Biosci* 13: 790-805

Nordberg E, Orlova A, Friedman M, Tolmachev V, Stahl S, Nilsson FY, Glimelius B & Carlsson J (2008) *In vivo* and *in vitro* uptake of 111In, delivered with the affibody molecule (ZEGFR:955)2, in EGFR expressing tumour cells. *Oncol Rep* 19: 853-857

Ogawa M, Kosaka N, Choyke PL & Kobayashi H (2009) *In vivo* molecular imaging of cancer with a quenching near-infrared fluorescent probe using conjugates of monoclonal antibodies and indocyanine green. *Cancer Res* 69: 1268-1272

Ogawa M, Regino CA, Choyke PL & Kobayashi H (2009) *In vivo* target-specific activatable near-infrared optical labeling of humanized monoclonal antibodies. *Mol Cancer Ther* 8: 232-239

Ogawa M, Regino CA, Seidel J, Green MV, Xi W, Williams M, Kosaka N, Choyke PL & Kobayashi H (2009) Dual-modality molecular imaging using antibodies labeled with activatable fluorescence and a radionuclide for specific and quantitative targeted cancer detection. *Bioconjug Chem* 20: 2177-2184

Okamoto I (2010) Epidermal growth factor receptor in relation to tumor development: EGFR-targeted anticancer therapy. *FEBS J* 277: 309-315

Orlova A, Magnusson M, Eriksson TL, Nilsson M, Larsson B, Hoiden-Guthenberg I, Widstrom C, Carlsson J, Tolmachev V, Stahl S & Nilsson FY (2006) Tumor imaging using a picomolar affinity HER2 binding affibody molecule. *Cancer Res* 66: 4339-4348

Orlova A, Nilsson FY, Wikman M, Widstrom C, Stahl S, Carlsson J & Tolmachev V (2006) Comparative *in vivo* evaluation of technetium and iodine labels on an anti-HER2

affibody for single-photon imaging of HER2 expression in tumors. *J Nucl Med* 47: 512-519

Orlova A, Tolmachev V, Pehrson R, Lindborg M, Tran T, Sandstrom M, Nilsson FY, Wennborg A, Abrahmsen L & Feldwisch J (2007) Synthetic affibody molecules: a novel class of affinity ligands for molecular imaging of HER2-expressing malignant tumors. *Cancer Res* 67: 2178-2186

Orlova A, Wallberg H, Stone-Elander S & Tolmachev V (2009) On the selection of a tracer for PET imaging of HER2-expressing tumors: direct comparison of a 124I-labeled affibody molecule and trastuzumab in a murine xenograft model. *J Nucl Med* 50: 417-425

Pal A, Glekas A, Doubrovin M, Balatoni J, Namavari M, Beresten T, Maxwell D, Soghomonyan S, Shavrin A, Ageyeva L, Finn R, Larson SM, Bornmann W & Gelovani JG (2006) Molecular imaging of EGFR kinase activity in tumors with 124I-labeled small molecular tracer and positron emission tomography. *Mol Imaging Biol* 8: 262-277

Panousis C, Rayzman VM, Johns TG, Renner C, Liu Z, Cartwright G, Lee FT, Wang D, Gan H, Cao D, Kypridis A, Smyth FE, Brechbiel MW, Burgess AW, Old LJ & Scott AM (2005) Engineering and characterisation of chimeric monoclonal antibody 806 (ch806) for targeted immunotherapy of tumours expressing de2-7 EGFR or amplified EGFR. *Br J Cancer* 92: 1069-1077

Pantaleo MA, Nannini M, Fanti S, Boschi S, Lollini PL & Biasco G (2009) Molecular imaging of EGFR: it's time to go beyond receptor expression. *J Nucl Med* 50: 1195-1196; author reply 1196, 1197

Pantaleo MA, Nannini M, Maleddu A, Fanti S, Nanni C, Boschi S, Lodi F, Nicoletti G, Landuzzi L, Lollini PL & Biasco G (2009) Experimental results and related clinical implications of PET detection of epidermal growth factor receptor (EGFr) in cancer. *Ann Oncol* 20: 213-226

Pectasides D, Gaglia A, Arapantoni-Dadioti P, Bobota A, Valavanis C, Kostopoulou V, Mylonakis N, Karabelis A, Pectasides M & Economopoulos T (2006) HER-2/neu status of primary breast cancer and corresponding metastatic sites in patients with advanced breast cancer treated with trastuzumab-based therapy. *Anticancer Res* 26: 647-653

Persson M, Tolmachev V, Andersson K, Gedda L, Sandstrom M & Carlsson J (2005) [(177)Lu]pertuzumab: experimental studies on targeting of HER-2 positive tumour cells. *Eur J Nucl Med Mol Imaging* 32: 1457-1462

Pines G, Kostler WJ & Yarden Y (2010) Oncogenic mutant forms of EGFR: lessons in signal transduction and targets for cancer therapy. *FEBS Lett* 584: 2699-2706

Regitnig P, Schippinger W, Lindbauer M, Samonigg H & Lax SF (2004) Change of HER-2/neu status in a subset of distant metastases from breast carcinomas. *J Pathol* 203: 918-926

Reilly RM, Kiarash R, Sandhu J, Lee YW, Cameron RG, Hendler A, Vallis K & Gariepy J (2000) A comparison of EGF and MAb 528 labeled with 111In for imaging human breast cancer. *J Nucl Med* 41: 903-911

Romond EH, Perez EA, Bryant J, Suman VJ, Geyer CE, Jr., Davidson NE, Tan-Chiu E, Martino S, Paik S, Kaufman PA, Swain SM, Pisansky TM, Fehrenbacher L, Kutteh LA, Vogel VG, Visscher DW, Yothers G, Jenkins RB, Brown AM, Dakhil SR,

Mamounas EP, Lingle WL, Klein PM, Ingle JN & Wolmark N (2005) Trastuzumab plus adjuvant chemotherapy for operable HER2-positive breast cancer. *N Engl J Med* 353: 1673-1684

Rosenthal EL, Kulbersh BD, King T, Chaudhuri TR & Zinn KR (2007) Use of fluorescent labeled anti-epidermal growth factor receptor antibody to image head and neck squamous cell carcinoma xenografts. *Mol Cancer Ther* 6: 1230-1238

Sampath L, Kwon S, Hall MA, Price RE & Sevick-Muraca EM (2010) Detection of Cancer Metastases with a Dual-labeled Near-Infrared/Positron Emission Tomography Imaging Agent. *Transl Oncol* 3: 307-317

Sampath L, Kwon S, Ke S, Wang W, Schiff R, Mawad ME & Sevick-Muraca EM (2007) Dual-labeled trastuzumab-based imaging agent for the detection of human epidermal growth factor receptor 2 overexpression in breast cancer. *J Nucl Med* 48: 1501-1510

Schechter NR, Wendt RE, 3rd, Yang DJ, Azhdarinia A, Erwin WD, Stachowiak AM, Broemeling LD, Kim EE, Cox JD, Podoloff DA & Ang KK (2004) Radiation dosimetry of 99mTc-labeled C225 in patients with squamous cell carcinoma of the head and neck. *J Nucl Med* 45: 1683-1687

Schechter NR, Yang DJ, Azhdarinia A, Kohanim S, Wendt R, 3rd, Oh CS, Hu M, Yu DF, Bryant J, Ang KK, Forster KM, Kim EE & Podoloff DA (2003) Assessment of epidermal growth factor receptor with 99mTc-ethylenedicysteine-C225 monoclonal antibody. *Anticancer Drugs* 14: 49-56

Schier R, McCall A, Adams GP, Marshall KW, Merritt H, Yim M, Crawford RS, Weiner LM, Marks C & Marks JD (1996) Isolation of picomolar affinity anti-c-erbB-2 single-chain Fv by molecular evolution of the complementarity determining regions in the center of the antibody binding site. *J Mol Biol* 263: 551-567

Simmons C, Miller N, Geddie W, Gianfelice D, Oldfield M, Dranitsaris G & Clemons MJ (2009) Does confirmatory tumor biopsy alter the management of breast cancer patients with distant metastases? *Ann Oncol* 20: 1499-1504

Simon R, Nocito A, Hubscher T, Bucher C, Torhorst J, Schraml P, Bubendorf L, Mihatsch MM, Moch H, Wilber K, Schotzau A, Kononen J & Sauter G (2001) Patterns of her-2/neu amplification and overexpression in primary and metastatic breast cancer. *J Natl Cancer Inst* 93: 1141-1146

Slamon DJ, Godolphin W, Jones LA, Holt JA, Wong SG, Keith DE, Levin WJ, Stuart SG, Udove J, Ullrich A & Press MF (1989) Studies of the HER-2/neu proto-oncogene in human breast and ovarian cancer. *Science* 244: 707-712

Smith-Jones PM, Solit DB, Akhurst T, Afroze F, Rosen N & Larson SM (2004) Imaging the pharmacodynamics of HER2 degradation in response to Hsp90 inhibitors. *Nat Biotechnol* 22: 701-706

Speake G, Holloway B & Costello G (2005) Recent developments related to the EGFR as a target for cancer chemotherapy. *Curr Opin Pharmacol* 5: 343-349

Steffen AC, Orlova A, Wikman M, Nilsson FY, Stahl S, Adams GP, Tolmachev V & Carlsson J (2006) Affibody-mediated tumour targeting of HER-2 expressing xenografts in mice. *Eur J Nucl Med Mol Imaging* 33: 631-638

Steffen AC, Wikman M, Tolmachev V, Adams GP, Nilsson FY, Stahl S & Carlsson J (2005) *In vitro* characterization of a bivalent anti-HER-2 affibody with potential for radionuclide-based diagnostics. *Cancer Biother Radiopharm* 20: 239-248

Stoscheck CM & King LE, Jr. (1986) Role of epidermal growth factor in carcinogenesis. *Cancer Res* 46: 1030-1037

Su H, Seimbille Y, Ferl GZ, Bodenstein C, Fueger B, Kim KJ, Hsu YT, Dubinett SM, Phelps ME, Czernin J & Weber WA (2008) Evaluation of [(18)F]gefitinib as a molecular imaging probe for the assessment of the epidermal growth factor receptor status in malignant tumors. *Eur J Nucl Med Mol Imaging* 35: 1089-1099

Tada H, Higuchi H, Wanatabe TM & Ohuchi N (2007) *In vivo* real-time tracking of single quantum dots conjugated with monoclonal anti-HER2 antibody in tumors of mice. *Cancer Res* 67: 1138-1144

Tang Y, Scollard D, Chen P, Wang J, Holloway C & Reilly RM (2005) Imaging of HER2/neu expression in BT-474 human breast cancer xenografts in athymic mice using [(99m)Tc]-HYNIC-trastuzumab (Herceptin) Fab fragments. *Nucl Med Commun* 26: 427-432

Tang Y, Wang J, Scollard DA, Mondal H, Holloway C, Kahn HJ & Reilly RM (2005) Imaging of HER2/neu-positive BT-474 human breast cancer xenografts in athymic mice using (111)In-trastuzumab (Herceptin) Fab fragments. *Nucl Med Biol* 32: 51-58

Tapia C, Savic S, Wagner U, Schonegg R, Novotny H, Grilli B, Herzog M, Barascud AD, Zlobec I, Cathomas G, Terracciano L, Feichter G & Bubendorf L (2007) HER2 gene status in primary breast cancers and matched distant metastases. *Breast Cancer Res* 9: R31

Tolmachev V, Friedman M, Sandstrom M, Eriksson TL, Rosik D, Hodik M, Stahl S, Frejd FY & Orlova A (2009) Affibody molecules for epidermal growth factor receptor targeting *in vivo*: aspects of dimerization and labeling chemistry. *J Nucl Med* 50: 274-283

Tolmachev V, Mume E, Sjoberg S, Frejd FY & Orlova A (2009) Influence of valency and labelling chemistry on *in vivo* targeting using radioiodinated HER2-binding Affibody molecules. *Eur J Nucl Med Mol Imaging* 36: 692-701

Tolmachev V, Nilsson FY, Widstrom C, Andersson K, Rosik D, Gedda L, Wennborg A & Orlova A (2006) 111In-benzyl-DTPA-ZHER2:342, an affibody-based conjugate for *in vivo* imaging of HER2 expression in malignant tumors. *J Nucl Med* 47: 846-853

Tolmachev V, Rosik D, Wallberg H, Sjoberg A, Sandstrom M, Hansson M, Wennborg A & Orlova A (2010) Imaging of EGFR expression in murine xenografts using site-specifically labelled anti-EGFR 111In-DOTA-Z EGFR:2377 Affibody molecule: aspect of the injected tracer amount. *Eur J Nucl Med Mol Imaging* 37: 613-622

Tran T, Engfeldt T, Orlova A, Widstrom C, Bruskin A, Tolmachev V & Karlstrom AE (2007) *In vivo* evaluation of cysteine-based chelators for attachment of 99mTc to tumor-targeting Affibody molecules. *Bioconjug Chem* 18: 549-558

Tran T, Orlova A, Sivaev I, Sandstrom M & Tolmachev V (2007) Comparison of benzoate- and dodecaborate-based linkers for attachment of radioiodine to HER2-targeting Affibody ligand. *Int J Mol Med* 19: 485-493

Tran TA, Ekblad T, Orlova A, Sandstrom M, Feldwisch J, Wennborg A, Abrahmsen L, Tolmachev V & Eriksson Karlstrom A (2008) Effects of lysine-containing mercaptoacetyl-based chelators on the biodistribution of 99mTc-labeled anti-HER2 Affibody molecules. *Bioconjug Chem* 19: 2568-2576

Tzahar E, Waterman H, Chen X, Levkowitz G, Karunagaran D, Lavi S, Ratzkin BJ & Yarden Y (1996) A hierarchical network of interreceptor interactions determines signal

transduction by Neu differentiation factor/neuregulin and epidermal growth factor. *Mol Cell Biol* 16: 5276-5287

Urano Y, Asanuma D, Hama Y, Koyama Y, Barrett T, Kamiya M, Nagano T, Watanabe T, Hasegawa A, Choyke PL & Kobayashi H (2009) Selective molecular imaging of viable cancer cells with pH-activatable fluorescence probes. *Nat Med* 15: 104-109

Velikyan I, Sundberg AL, Lindhe O, Hoglund AU, Eriksson O, Werner E, Carlsson J, Bergstrom M, Langstrom B & Tolmachev V (2005) Preparation and evaluation of (68)Ga-DOTA-hEGF for visualization of EGFR expression in malignant tumors. *J Nucl Med* 46: 1881-1888

Vincent-Salomon A, Pierga JY, Couturier J, d'Enghien CD, Nos C, Sigal-Zafrani B, Lae M, Freneaux P, Dieras V, Thiery JP & Sastre-Garau X (2007) HER2 status of bone marrow micrometastasis and their corresponding primary tumours in a pilot study of 27 cases: a possible tool for anti-HER2 therapy management? *Br J Cancer* 96: 654-659

Weissleder R (2001) A clearer vision for *in vivo* imaging. *Nat Biotechnol* 19: 316-317

Weissleder R & Pittet MJ (2008) Imaging in the era of molecular oncology. *Nature* 452: 580-589

Wikman M, Steffen AC, Gunneriusson E, Tolmachev V, Adams GP, Carlsson J & Stahl S (2004) Selection and characterization of HER2/neu-binding affibody ligands. *Protein Eng Des Sel* 17: 455-462

Wikstrand CJ, Reist CJ, Archer GE, Zalutsky MR & Bigner DD (1998) The class III variant of the epidermal growth factor receptor (EGFRvIII): characterization and utilization as an immunotherapeutic target. *J Neurovirol* 4: 148-158

Willmann JK, van Bruggen N, Dinkelborg LM & Gambhir SS (2008) Molecular imaging in drug development. *Nat Rev Drug Discov* 7: 591-607

Xu N, Cai G, Ye W, Wang X, Li Y, Zhao P, Zhang A, Zhang R & Cao B (2009) Molecular imaging application of radioiodinated anti-EGFR human Fab to EGFR-overexpressing tumor xenografts. *Anticancer Res* 29: 4005-4011

Yang L, Mao H, Wang YA, Cao Z, Peng X, Wang X, Duan H, Ni C, Yuan Q, Adams G, Smith MQ, Wood WC, Gao X & Nie S (2009) Single chain epidermal growth factor receptor antibody conjugated nanoparticles for *in vivo* tumor targeting and imaging. *Small* 5: 235-243

Yarden Y & Sliwkowski MX (2001) Untangling the ErbB signalling network. *Nat Rev Mol Cell Biol* 2: 127-137

Yeh HH, Ogawa K, Balatoni J, Mukhapadhyay U, Pal A, Gonzalez-Lepera C, Shavrin A, Soghomonyan S, Flores L, 2nd, Young D, Volgin AY, Najjar AM, Krasnykh V, Tong W, Alauddin MM & Gelovani JG (2011) Molecular imaging of active mutant L858R EGF receptor (EGFR) kinase-expressing nonsmall cell lung carcinomas using PET/CT. *Proc Natl Acad Sci U S A* 108: 1603-1608

Zhang X, Silva E, Gershenson D & Hung MC (1989) Amplification and rearrangement of c-erb B proto-oncogenes in cancer of human female genital tract. *Oncogene* 4: 985-989

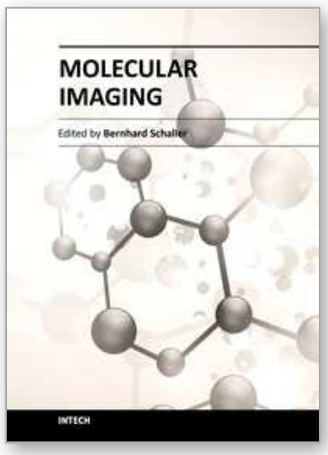

Molecular Imaging

Edited by Prof. Bernhard Schaller

ISBN 978-953-51-0359-2
Hard cover, 390 pages
Publisher InTech
Published online 16, March, 2012
Published in print edition March, 2012

The present book gives an exceptional overview of molecular imaging. Practical approach represents the red thread through the whole book, covering at the same time detailed background information that goes very deep into molecular as well as cellular level. Ideas how molecular imaging will develop in the near future present a special delicacy. This should be of special interest as the contributors are members of leading research groups from all over the world.

How to reference

In order to correctly reference this scholarly work, feel free to copy and paste the following:

Haibiao Gong, Lakshmi Sampath, Joy L. Kovar and D. Mike Olive (2012). Targeting EGFR and HER2 for Molecular Imaging of Cancer, Molecular Imaging, Prof. Bernhard Schaller (Ed.), ISBN: 978-953-51-0359-2, InTech, Available from: http://www.intechopen.com/books/molecular-imaging/targeting-egfr-and-her2-for-molecular-imaging-of-cancer

INTECH
open science | open minds

InTech Europe
University Campus STeP Ri
Slavka Krautzeka 83/A
51000 Rijeka, Croatia
Phone: +385 (51) 770 447
Fax: +385 (51) 686 166
www.intechopen.com

InTech China
Unit 405, Office Block, Hotel Equatorial Shanghai
No.65, Yan An Road (West), Shanghai, 200040, China
中国上海市延安西路65号上海国际贵都大饭店办公楼405单元
Phone: +86-21-62489820
Fax: +86-21-62489821

IntechOpen